



Facilitated transport of CO₂ in novel PVAm/PVA blend membrane

Liyuan Deng, Taek-Joong Kim, May-Britt Hägg*

Department of Chemical Engineering, Faculty of Natural Sciences and Technology, Norwegian University of Science and Technology (NTNU), NO-7491 Trondheim, Norway

ARTICLE INFO

Article history:

Received 19 August 2008

Received in revised form 21 April 2009

Accepted 17 May 2009

Available online 23 May 2009

Keywords:

Blend membrane
Facilitated transport
Fixed-site-carrier
Polyvinyl amine
Polyvinyl alcohol

ABSTRACT

A defect-free ultra thin PVAm/PVA blend facilitated transport membrane cast on a porous polysulfone (PSf) support was developed and evaluated in this study. The target membrane was prepared from commercial polyvinyl amine (PVAm) and polyvinyl alcohol (PVA). Effects of experimental conditions were investigated for a CO₂-N₂ mixed gas. A CO₂/N₂ separation factor of up to 174 and a CO₂ permeance up to 0.58 m³(STP)/(m² h bar) were documented. Experimental results suggest that CO₂ is being transported according to the facilitated transport mechanism through this membrane. The fixed amino groups in the PVAm matrix function as CO₂ carriers to facilitate the transport whereas the PVA adds mechanical strength to the blend by entanglement of the polymeric chains hence creating a supporting network. The good mechanical properties obtained from the blend of PVA with PVAm, enabled an ultra thin selective layer (down to 0.3 μm) to be formed on PSf support (with MWCO of 50,000), resulted in both high selectivity and permeance. The PVAm/PVA blend membrane also exhibited a good stability during a 400 h test.

© 2009 Elsevier B.V. All rights reserved.

1. Introduction

Concern for the changing climate and emission of greenhouse gases, especially CO₂, has resulted in the acceleration of innovative solutions for CO₂ capture and sequestration, among various membrane solutions. Using membranes for CO₂ capture will be an environmental friendly process, as well as a low cost and energy saving process, if a membrane with high flux and selectivity is chosen. Such membranes may be those with enhanced transport for selected gases. Membranes may be prepared from various types of materials, but currently only polymeric membranes are commercially available for gas separation. Polymers may easily be prepared as hollow fibers or spiral-wound modules with high packing density (m²/m³), and will be the best option for large volume gas streams in industry. Among the new materials with a very promising potential for highly efficient gas separation are the facilitated transport membranes, which exhibit both high permeability and high selectivity compared to the conventional polymeric membranes. In facilitated transport the flux of a permeant gas is selectively enhanced by means of a reversible reaction between the active permeant gas and the carrier, whereas other gases inert to the carriers, such as H₂, N₂ and CH₄, will permeate exclusively by the solution-diffusion mechanism.

Scholander [1] demonstrated a facilitated transport membrane for the first time in 1960. A supported liquid membrane (SLM) was

reported with hemoglobin as oxygen facilitated transport carriers, showing remarkably high selectivity in favor of O₂. Numerous studies of SLM have been carried out thereafter [1–5]. However, serious degradation problems, such as evaporation of solution and deactivation of the complexing agent (carrier), restricted its further development and application. In 1980 an ion exchange membrane was firstly reported by LeBlanc et al. [2] to overcome the problems of SLMs, in which facilitated carriers were kept within the membrane matrix using electrostatic forces and hence the degradation of carriers was minimized. As another approach to fix the carriers, Matsuyama et al. [6–8] applied plasma technology to introduce the desired functional groups, and obtained membranes which showed remarkably high CO₂ permeability and selectivity over CH₄ and N₂. Since 1994 Quinn et al. [9–14] published and patented a series of polyelectrolyte membranes or polyelectrolyte-salt blend membranes for acid gas separation. Nevertheless, none of the above membranes has yet been commercialized, which may be due to their instability problems and scale-up limitations.

From the point of stability, polymeric fixed-site-carrier (FSC) membranes are in general more favorable than membranes with mobile carriers since the carriers in FSC membrane are covalently bonded directly to the polymer matrix. Yoshikawa et al. [15,16] synthesized a polymeric membrane having pyridine moiety or amine moiety, and confirmed an acid–base interaction between CO₂ and fixed carriers. Zhang [17,18] reported a new composite membrane containing two kinds of CO₂ carriers synthesized through the hydrolysis of polyvinylpyrrolidone (PVP) and Matsuyama et al. [19] reported a polyethylenimine/poly(vinyl alcohol) (PEI/PVA) blend membrane with fixed carriers. Recently Ho and co-workers [20,21] published their results on CO₂ separation from H₂, N₂ and CO by a

* Corresponding author. Tel.: +47 73594033; fax: +47 73594080.
E-mail address: hagg@nt.ntnu.no (M.-B. Hägg).

polyallylamine (PAAm), amino acid salt, potassium hydroxide and PVA blend membrane, which was claimed to contain both mobile and fixed carriers. Cai et al. [22] also reported a PAAm/PVA blend membrane with selectivities for CO₂ over N₂ and CO₂ over CH₄ of 80 and 58, respectively. Kim et al. [23] prepared a composite polyvinyl amine (PVAm) membrane for CO₂ capture. The membrane was prepared from in-house synthesized PVAm with a high molecular weight (MW 80,000) on a PSf porous support, and showed a very high ideal selectivity of pure CO₂ over CH₄ (>1000). A comprehensive review article on facilitated transport membranes has been published by Hägg and Quinn [24]. A mechanism of facilitated gas transport in fixed-site-carrier membranes has been presented by Noble et al. [4,25–27].

As a hydrogel with sufficient primary amino groups, PVAm exhibits high CO₂ selective absorbability. In the water-swollen FSC membrane containing sufficient amino groups, CO₂ is mediated based on the similar reactions as in mobile carrier membranes although the amino groups are fixed to the membrane matrix. Water is also playing a role in the CO₂ transport when swelling the membranes. Some researchers [8,17,18,28,29] suggested that CO₂ reacts with the carriers (e.g. primary amino groups) and water to produce amine–CO₂–H₂O complexes (e.g. RNHCOO[−]) and HCO₃[−] within the membrane, diffusing in the form of HCO₃[−] ions, as shown in Eq. (1). This is believed to be what makes it possible to obtain the high CO₂ selectivity and permeability comparable to those of mobile carrier membranes.



The weak basic amino group will initiate the reaction. However, considering that amino groups are not consumed during the reversible reactions, they are taking the role of catalysts for the reversible CO₂ hydration reactions, the final reactions can therefore be demonstrated with Eq. (2):



Wang et al. [17,29,30] confirmed the reaction of CO₂ with water and the form of HCO₃[−] in water-swollen pentaerythritol tetraethylenediamine (PETEDA) membranes by Fourier transform-infrared spectroscopy (FTIR) using attenuated total reflectance (ATR) techniques. They documented that new bands assigned to HCO₃[−] and the complex of CO₂ and amino moieties in PETEDA appeared in the spectrum of the membrane absorbed CO₂, while in the wet membrane contacted with only CH₄, no new band or shift of wave numbers were displayed.

The aim of this study has been to tailor an economically and technically viable polymeric membrane for CO₂ capture. The demands for this membrane include: good mechanical strength, long time stability, high separation performance, cheap and a simple fabrication process.

A mechanically PVA-like PVAm/PVA blend membrane was developed to meet the above demands. The membrane was prepared from a commercial PVAm (delivered as PVAm HCl) with a molecular weight of 25,000. With such a low MW, a swollen PVAm membrane will usually be sticky and resemble a fluid of high viscosity, hence it is impossible to form a thin selective layer. It was, however, believed that blending of the PVAm with a more mechanically robust polymer could be a solution to this problem, and polyvinyl alcohol (PVA) was selected as the component for blending. PVA is also a hydrogel with excellent film forming properties, resistant to oil, grease and most of organic solvents, exhibiting high tensile strength and flexibility. Water can act as a plasticiser and reduce the tensile strength of PVA, but also increase its elongation and tear strength. PVA chains are stretched and more flexible when heated above *T_g* (85 °C) [31].

An assumed schematic illustration of the PVAm and PVA blend was given in Fig. 1. In this study, the commercial PVAm (MW 25,000)

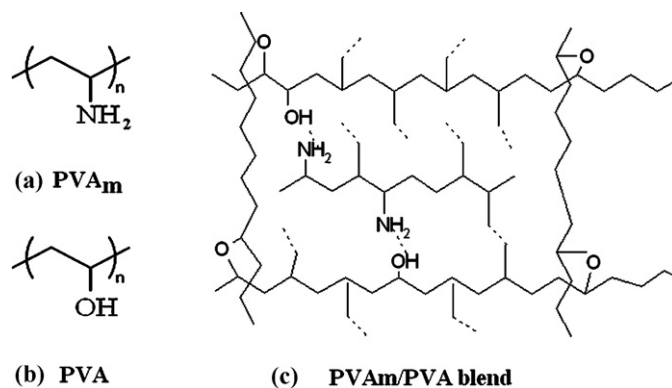


Fig. 1. Schematic diagram of PVAm/PVA blend polymer framework.

was entangled with and fixed inside the PVA chain network to offer CO₂ facilitated carriers. The chlorine (Cl[−]) from the commercial PVAm HCl may also offer highly polar sites in the membrane, which may restrict the permeation of non-polar gases while favor that of polar gases. DSC measurements confirmed that a homogenous blend was obtained, and FTIR and XPS analysis confirmed that the blended PVA and PVAm were cross-linked by heating in the range of 90–120 °C. The heat treatment would also cause some physical cross-linking by some rearrangement of crystallites in the polymer matrix. With an abundance of amino groups within the blended polymer matrix, the target membrane showed high selectivity and CO₂ permeability while maintaining good mechanical properties in a water swelling operation condition.

2. Experimental

2.1. Preparation of PVAm/PVA blend membrane

The PVAm/PVA blend membrane was prepared as a composite membrane with a thin selective layer of this homogenous blend on a PSf ultrafiltration membrane (Alfa Laval, MWCO 50,000). The PSf support was rinsed with dilute NaOH solution and flushed with water to remove any possible contaminants from supplier before use. The polymer solution of PVAm/PVA blend was prepared by adding PVA (90% hydrolyzed powder, Merck Schuchart, MW 72,000) aqueous solution to a PVAm (polyvinylamine hydrochloride, Polyscience, Inc., MW 25,000) aqueous solution of the same concentration. Both PVAm and PVA were used as received. The pH values of the PVA and PVAm solutions are 5.0 and 4.5, respectively. The composition of the blend solution was determined by adjusting the weight ratio of above solutions. All membranes reported here were of the same optimized blend ratio except otherwise indicated. After stirring the mixture overnight and ultrasonic mixing for 2 min, the polymer solution was then cast onto a PSf substrate with a calculated amount of blend solution to give the desired thickness. After casting, the membrane was dried in an oven at 45 °C for 5 h. All membranes were cross-linked by heating to 90–120 °C for 1 h in a convection oven.

2.2. Membrane characterization

The thermal properties of the PVAm, PVA and PVAm/PVA blend were measured on a TA Q100 differential scanning calorimeter (DSC). A method with a ‘freeze–heat–freeze–heat’ cycle was designed to minimize the influence of the absorbed water in the samples. The temperature range scanned was from −85 °C to 300 °C at a heating rate of 20 °C/min. The cross-section and surface of the membranes were examined using field emission scanning electron microscopy (FESEM, Zeiss Ultra 55 Limited Edition). Cross-sectional

samples were prepared by fracturing the membranes in liquid nitrogen. Samples were coated with carbon under vacuum before observation. FTIR spectra of PVAm, PVA and PVAm/PVA blends before and after heat treatment for cross-linking were scanned ($4000\text{--}400\text{ cm}^{-1}$) on a Thermo Nicolet FTIR Nexus Spectrophotometer. X-ray photoelectron spectroscopy (XPS) equipped with monochromatized Al $K\alpha$ X-ray source (GammaData Scienta) and hemispherical SES 2002 electron energy analyzer was performed to investigate the membrane surface composition. Wide-angle X-ray diffraction (WAXD) patterns of the top layers ($1.0\ \mu\text{m}$) of the heated and non-heated blend membrane samples were recorded with a Cu $K\alpha$ radiation produced by a Bruker AXS D8Focus X-ray. The tensile strength and elongation at break (ϵ_b) for membrane materials were determined on an electronic tensile testing machine (LR10K). The gauge length was 10–20 mm and cross head speed was 1–50 mm/min. All samples were tested at room temperature and 37.5% relative humidity. The degree of water swelling of PVAm/PVA blend was determined by weighing the dry sample and the sample conditioned in a glass vessel saturated with water vapour. This procedure was repeated until the film reached a constant weight (equilibrium water uptake). The water swelling degree (SD) of membrane was calculated according to the following equation:

$$\text{SD}(\%) = \frac{W_s - W_d}{W_d} \times 100 \quad (3)$$

where W_s and W_d are the masses of the swollen and dry membranes, respectively.

2.3. Permeation experiments

Separation performances of membranes were tested in a gas permeation rig (see Fig. 2). Feed gases were supplied from a pre-mixed gas cylinder (10 vol.% of CO_2 in CO_2/N_2 gas mixture, AGA AS). A flat sheet type membrane module was mounted in a thermostatic cabinet with a temperature control system. A membrane (diameter of 50 mm) was sandwiched between the permeate chamber and the feed gas chamber, supported by a porous metal disk and sealed with rubber O-rings. Both feed gas and sweep gas were saturated with water vapour by bubbling through water bottles. A bypass line with a precise valve paralleling with the upstream

water bubbling bottle was attached to adjust the humidity of feed gas. Flow rate and pressure were recorded and controlled by a flow controller, flow indicator and pressure transmitters (MKS) respectively and logged directly into a computer (by Labview). Relative humidity of feed gas was measured online by a humidity analyser. The composition of the permeate gas was analyzed online by a gas chromatograph equipped with a thermal conductivity detector (MicroGC3000). Some operation conditions, such as feed gas flow rate, relative humidity, feed pressure, were varied to investigate their respective effects on the membrane performance.

A sweep gas was used on permeate side (He or N_2 indicated in Fig. 2) for better recording of fluxes and gas compositions. Permeance of a species i was defined as the flux divided by the partial pressure differences between the upstream and downstream of the membrane and reported in units of $[\text{m}^3(\text{STP})/(\text{m}^2\ \text{h bar})]$ and given the symbol R_i . The selectivity (α) was calculated from permeance of CO_2 , R_{CO_2} and N_2 , R_{N_2} , as expressed in Eq. (4) [32,33].

$$\alpha = \frac{R_{\text{CO}_2}}{R_{\text{N}_2}} \quad (4)$$

$\text{CO}_2\text{--N}_2$ (10 vol.% CO_2) mixed gas was used as feed gas. Permeation experiments were carried out at $25\ ^\circ\text{C}$ with a feed pressure varying from 2 bar to 15 bar, and separation performance was recorded when the system had been stabilized.

3. Results and discussion

3.1. Membrane characteristics

The defect-free ultra thin homogeneous PVAm/PVA blend membranes cast on a microporous PSf supports were characterized. The DSC graph of the PVAm/PVA blend in Fig. 3 shows only one melting point (T_m) and is different from those of PVAm and PVA; this should suggest that PVAm and PVA are compatible and mixed on a molecular level. A homogeneous blend has been obtained. Solvent (water in this case) contained in polymer can to some extent cause the melting point depression, so a freeze–heat cycle from $-85\ ^\circ\text{C}$ to $240\ ^\circ\text{C}$ was designed as a pre-treatment before the scanning from $-85\ ^\circ\text{C}$ to $300\ ^\circ\text{C}$ to extract water vapour from the samples. Since both PVA and PVAm are highly crystalline (especially PVAm), no

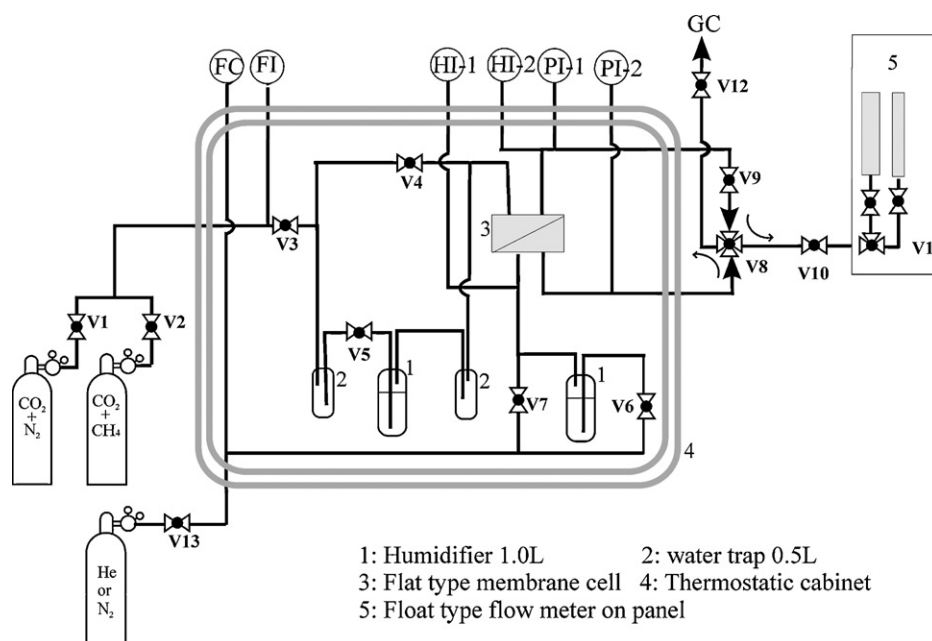


Fig. 2. Experimental set-up for mixed gas permeation testing.

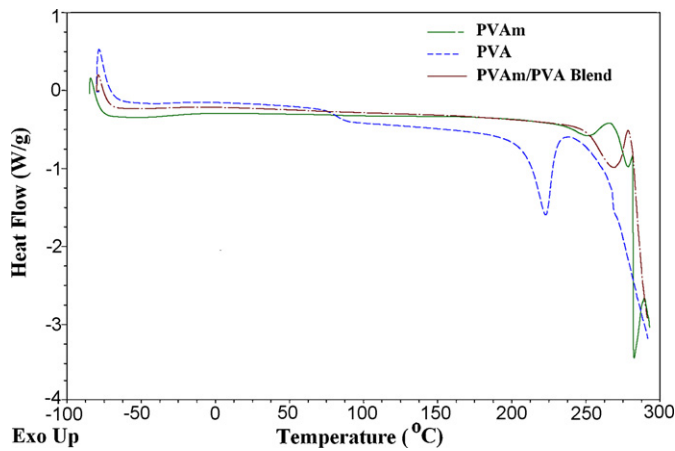


Fig. 3. DSC curves of PVAm, PVA and PVAm/PVA blend.

apparent T_g was found in PVAm samples or in the blend samples [34].

When casting a small amount of hydrophilic PVAm aqueous solution on hydrophobic PSf support (contact angle in water is $52.4 \pm 2.4^\circ$) [35], the solution was not able to smoothly wet the support surface and to form continuous solution layer, but drops, due to the big surface tension of the solution on the support. Benefiting from the hydrophobic groups ($-\text{OCCH}_3$) in the partially hydrolyzed PVA (90% hydrolyzed), the amphiphilic PVA in the PVAm/PVA blend aqueous solution functioned as surfactants that can reduce the surface tension and offer a good contact between the hydrophilic solution and the hydrophobic surface, enabling the formation of the defect-free ultra thin coating on PSf support. The cross-section of the composite membrane in the SEM image in Fig. 4 shows the PVAm/PVA blend as a selective layer with thickness of $0.5 \mu\text{m}$. No evident 'pore-filling' phenomena were found from the image even though this membrane had endured measurements at 15 bar pressure. Since a sudden depressurization would cause serious damage to the coating layer by the explosion of the quickly evaporated water bubbles, the membrane thickness was measured after being gradually depressurized to atmosphere and equilibrated in highly humidified environment. The thickness of the coating layer was about the same as the one calculated. The strong PVA chain bridging over pores may help stopping small PVAm chains from leaking into pores. Permeation data reported in this paper also confirmed the non-pore-filling feature of the blend membrane.

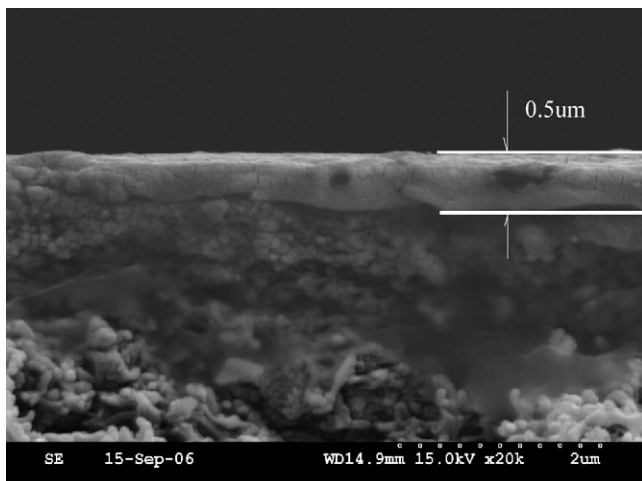


Fig. 4. SEM image of PVAm/PVA blend membrane cross-section.

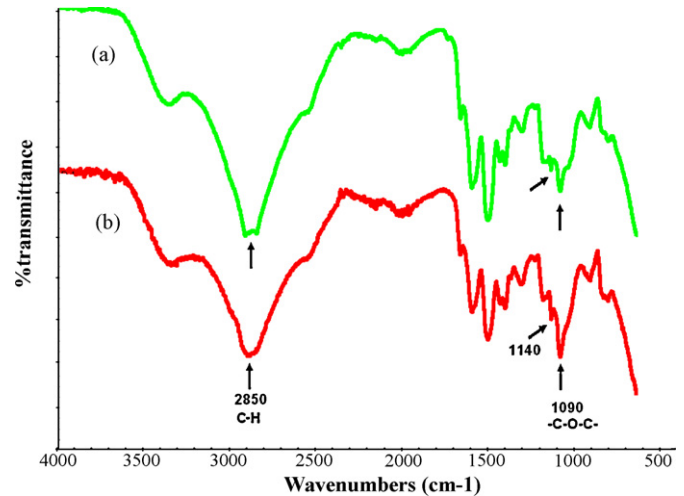


Fig. 5. FTIR spectra of PVAm/PVA blend before (a) and after (b) cross-linked by heating.

Pure PVAm, however, has a tendency to pore filling at higher pressures [23].

Fig. 5 represents the FTIR spectra of PVAm/PVA blends before and after heat cross-linking. Unlike the type of cross-linking reactions initiated by cross-linking agents, the heat cross-linking reactions are relatively weak. No evident new peaks or wave number shifts were observed in IR spectrum. The major chemical structures before and after heating are similar. However, the intensity of the peak at 1090 cm^{-1} in the FTIR spectrum was evidently increased from lower than that of the peak at 1500 cm^{-1} and 1610 cm^{-1} (assigned to $-\text{NH}_2$, $-\text{N}-\text{H}$ and $-\text{C}-\text{N}-$ respectively) to apparently higher than them, suggesting a change of polymer structure during heating. The band near 1090 cm^{-1} can be assigned to the combination of $-\text{C}-\text{O}-\text{C}-$ bond and $\equiv\text{C}-\text{OH}$ bond [36–38]. Combining with the XPS analysis, the increase of the intensity of peak at 1090 cm^{-1} can be attributed to the form of $-\text{C}-\text{O}-\text{C}-$ structure after heat cross-linking. The XPS spectra and atomic ratio of carbon, oxygen in unheated (a) and heat cross-linked (b) PVAm/PVA blend membrane are shown in Fig. 6. The content of oxygen in the blend membrane increases from 18% to 22% after being cross-linked by heating, which also suggested the forming of cross-linking chain ($-\text{C}-\text{O}-\text{C}-$) in the blend network. The characteristic crystallization-sensitive band of PVA at 1140 cm^{-1} undergoes a change in the

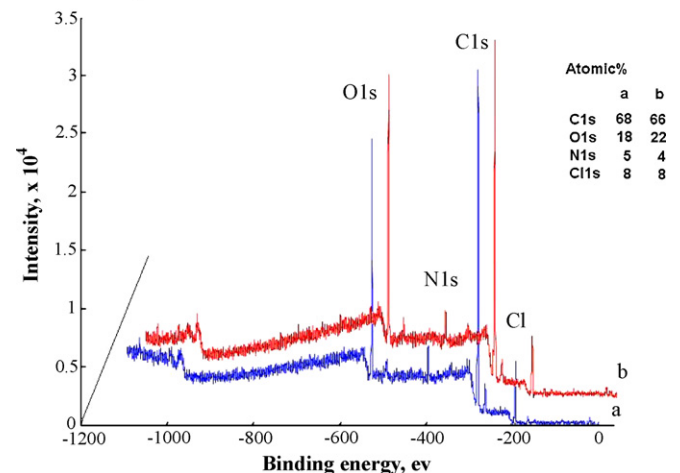


Fig. 6. XPS spectra of unheated (a) and heat cross-linked (b) PVAm/PVA blend membrane.

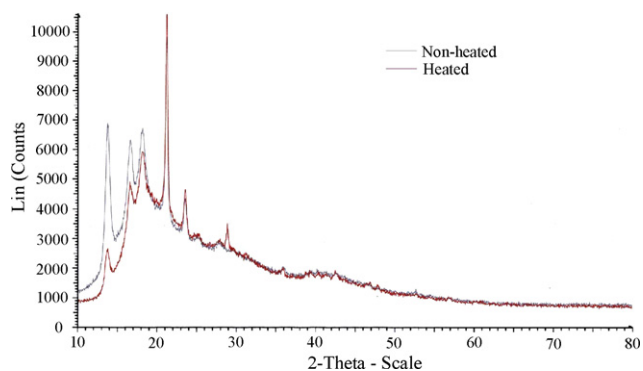


Fig. 7. XRD spectra of unheated and heat cross-linked PVAm/PVA blend membrane.

heated sample, indicating that cross-linking by heating may have caused physical cross-linking by the rearrangement of the crystal regions of the blend [36,39]. The different pattern of WAXD spectra of the samples with and without heat cross-linking confirmed the change of the crystal structures, as can be seen in Fig. 7. The drop of the peak intensities (at $2\theta = 13.5, 16.5$ and 18) after heat cross-linking in WAXD patterns indicate that the relative crystallinity in the blend membrane decreases. However, the chemical structure of the heat cross-linked PVAm/PVA blend is complicated – no apodictic structure can be determined only based on the current characterizations.

The enhancement to mechanical strength by blending PVA with PVAm and the heat cross-linking of the blend was also apparent by pure observation. The membrane prepared from PVAm (MW 25,000) was brittle in the dry state and changed to a sticky viscous form in water-swollen state (the state of the membrane during separation). The addition of PVA significantly improved the mechanical strength of the membrane. In the dry state the blended membrane was more flexible as compared with pure PVAm membrane, while after water swelling the blended membrane exhibited sufficient strength and elongation. The average tensile strength for PVAm/PVA blend samples of 60.53 MPa and elongations at break (ϵ_b) of 8.46% were determined. The PVA samples exhibited a relatively higher tensile strength of 84 MPa and a lower elongation at break of 4.8%, while PVAm samples were too fragile to be tested at the same conditions.

Water swelling behavior of the blend membranes was investigated based on orthogonal experimental design L_9 (3^4) [40]. The four selected factors were the percentage of PVA in PVAm/PVA blend, heat cross-linking temperature, heating time and a blank column as reference. Rough trends of the effects on membrane swelling capacity are given in Fig. 8, where I, II and III represent low, medium and high levels, which are 90°C as low and 120°C as high level in cross-linking temperature, 30 min as low and 90 min as high level in heating duration and 20% as low and 60% as high level in PVA percentage in Fig. 8(a), (b) and (c), respectively. The analysis of the orthogonal test showed the rough trends of the effects of the factors. The effect of cross-linking temperature on the degree

of swelling exhibits an optimum condition at level 2, as shown in Fig. 8(a). Heating beyond the optimal temperature resulted in a poorer membrane swelling capacity. This indicates the formation of an efficient polymeric network by heat activated cross-linking at the optimal temperature. Over heating may result in too strong cross-linking, and therefore the loss of membrane swelling capacity. The effect of the duration of heating is plotted in Fig. 8(b). Swelling capacity of the membrane increases as the duration of heating increases in the testing range. However, there is significant interaction between heating temperature and duration. A single factor experiment was carried by varying the duration of heating at the optimized temperature (level II). The degree of swelling was no longer increasing with the duration of heating longer than level III in the investigated range. The optimized strategy of cross-linking temperature and duration of heating (at level III) was determined by the combination of the analysis of the orthogonal and single factor experiment results. Fig. 8(c) shows that the swelling degree declined significantly with the increase of PVA percentage. To optimize the PVAm/PVA ratio, the effect of PVA percentage in the blend was also investigated on single factor experiment by varying the PVA percentage at the optimized heating temperature and duration. Results exhibit an optimal value at 20% PVA. Even though PVAm has a higher water affinity than PVA, the addition of 20% of PVA slightly increases the blend's swelling capacity. A stronger network offered by the entanglement of PVA with PVAm chains may efficiently retain water within the polymer matrix and hence the membrane may reach a higher degree of water swelling.

3.2. Permeation characteristics

The CO_2 separation performance of the PVAm/PVA blend membrane is strongly dependent on humidity. The selective layer thickness and operation pressure also affected the CO_2 transport. Their respective effects are in good accordance with the characteristic of facilitated transport mechanism.

3.2.1. Effect of relative humidity

Fig. 9 illustrates the effects of relative humidity on CO_2 permeance and CO_2/N_2 selectivity of a PVAm/PVA blend membrane with a selective layer of $0.3\ \mu\text{m}$ at process conditions of 2 bar and 25°C . In the measured relative humidity range, both the CO_2/N_2 selectivity and CO_2 permeance showed a monotonously rise with increasing relative humidity. A remarkable CO_2/N_2 selectivity of 174 was recorded at the highest humidity as indicated in Fig. 9(a). It is obvious that high relative humidity enables a higher degree of membrane swelling, which favors both CO_2 and N_2 transport in the membrane, however, the transport mechanisms differ. This results in a big difference in the increase of CO_2 and N_2 permeance with the increase of relative humidity from 50% to 92%. As can be seen in Fig. 9(b), the CO_2 permeance increased dramatically from $0.05\ \text{m}^3(\text{STP})/(\text{m}^2\ \text{h bar})$ to $0.58\ \text{m}^3(\text{STP})/(\text{m}^2\ \text{h bar})$, whereas N_2 permeance increased from $0.009\ \text{m}^3(\text{STP})/(\text{m}^2\ \text{h bar})$ to $0.03\ \text{m}^3(\text{STP})/(\text{m}^2\ \text{h bar})$. In dry condition the permeances of both CO_2 and N_2 were approximately $0.001\ \text{m}^3(\text{STP})/(\text{m}^2\ \text{h bar})$. Almost no selectivity was recorded. This is probably due to the high crystallinity of the PVAm and PVA in dry state.

The characteristic of the strong humidity dependence of CO_2 transport suggests that CO_2 follows facilitated transport mechanism in the water-swollen PVAm/PVA blend membrane [23]. It is reasonable to assume that when the membranes are in highly water-swollen conditions, Cl^- become mobile and is no longer bonded to the amino groups. When the pH value of the PVAm solution is 4.5 (as was used in this study), the free amino group is approximately 50% [34]. These free primary amino groups are hence free to function as the CO_2 facilitated carriers, as indicated in Eq. (1). Gas CO_2 dissolves in the membrane, forming the amine- CO_2 - H_2O

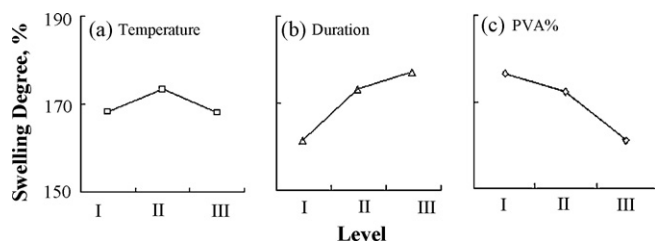


Fig. 8. Effects of heat cross-linking temperature (a), duration (b) and PVA% (c) on the degree of membrane swelling.

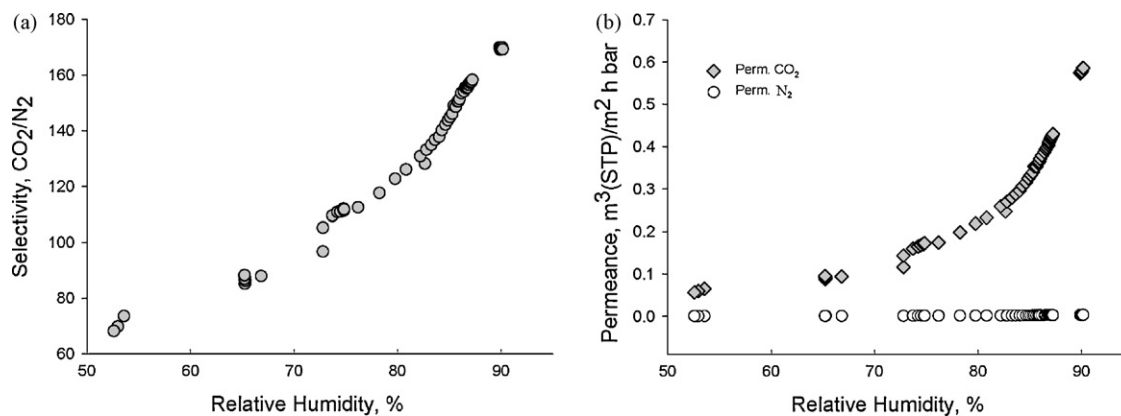


Fig. 9. Effects of relative humidity on CO₂ separation performance, selective layer of 0.3 μm , sweep gas flow rate 0.08 ml/s, at 2 bar, 25 °C.

complex and finally bicarbonate ion HCO_3^- , and permeating in the swollen polymer matrix by ‘jumping’ from one amino site to another. Hence the CO₂ transport through this PVAm/PVA blend membrane will follow three steps: (1) dissolution and reaction of CO₂ with water and amino groups to form CO₂-carrier complex and HCO_3^- at feed side, (2) diffusion of HCO_3^- through the membrane, and (3) decomposition of HCO_3^- and desorption of CO₂ at permeate side. The diffusion coefficient of the ion in liquid is normally four orders of magnitude greater than that of gases in solid [41], while in solvent swollen or gel system, the diffusivity can be calculated. Matsuyama et al. [42] have given equations based on the free volume theory to calculate the diffusion coefficient of a water-swollen gel. The $D_{\text{gel}}/D_{\text{water}}$ is found to increase with the increase of the degree of water swelling, water volume fraction in gel membrane, the affinity of solute, etc. It is hence believed that CO₂ forms the ion HCO_3^- when diffusing through this water-swollen FSC membrane, and hence the membrane exhibits very high CO₂ permeance and consequently high selectivity of CO₂ over N₂.

However, when thicker membranes (2.5–35 μm) were tested, a slight CO₂/N₂ selectivity drop was observed at a high relative humidity of around 90%. The loosening of polymer structure by over swelling at high relative humidity reduces the sieving capability of the membrane. Good cross-linking is very important to ensure an efficient selective structure of the membrane.

3.2.2. Effect of feed pressure

Fig. 10 shows the separation performance of the PVAm/PVA blend membrane with a selective layer of 0.5 μm at different feed pressures. CO₂/N₂ selectivity up to 150 at 2 bar was achieved with permeance of 0.43 m³(STP)/(m² h bar) whereas permeance of

0.11 m³(STP)/(m² h bar) was reached with a selectivity of 112 at 15 bar. As can be seen in Fig. 10(a), the CO₂/N₂ selectivity of the blend membrane decreases with feed pressure increasing from 2 bar to 15 bar. When above 5 bar the decreasing trend relaxes and the selectivity of CO₂/N₂ becomes almost constant. Fig. 10(b) shows that both the permeance of CO₂ and N₂ decrease with increasing feed pressure, but their trends are different. The different trends for CO₂ and N₂ permeance suggest that the transport of CO₂ and N₂ through membrane follows different transport mechanisms.

As a characteristic of facilitated transport, membrane permeance will generally decrease in the beginning with increasing feed partial pressure due to the saturation of carriers. When the carriers are saturated, the permeance will stabilize and solution-diffusion takes over. At low feed pressure (2–5 bar) the CO₂ permeance decreases rapidly with increasing feed pressure whereas the N₂ permeance is nearly constant. At feed pressures 5–15 bar, however, CO₂ permeance keeps nearly constant whereas N₂ permeance decreases significantly. This may be due to the increase of diffusion resistance of gases in the packed and hence less water swelled membrane at higher pressure. It is believed that the hindrance of polar Cl⁻ sites towards the permeation of the non-polar N₂ gas becomes more obvious when membrane is less swelled, which may also contribute to the decrease of N₂ permeance at high pressure. Packing effect in the water swelling polymer can be described as the decrease of the free volume occupied by water, not the same as the packing of the polymer matrix in dry state. To conclude, the trend of CO₂ permeance exhibited the characteristic of facilitated transport mechanism as expected, whereas N₂ transport is apparently under restricted solution-diffusion mechanism in this membrane [4].

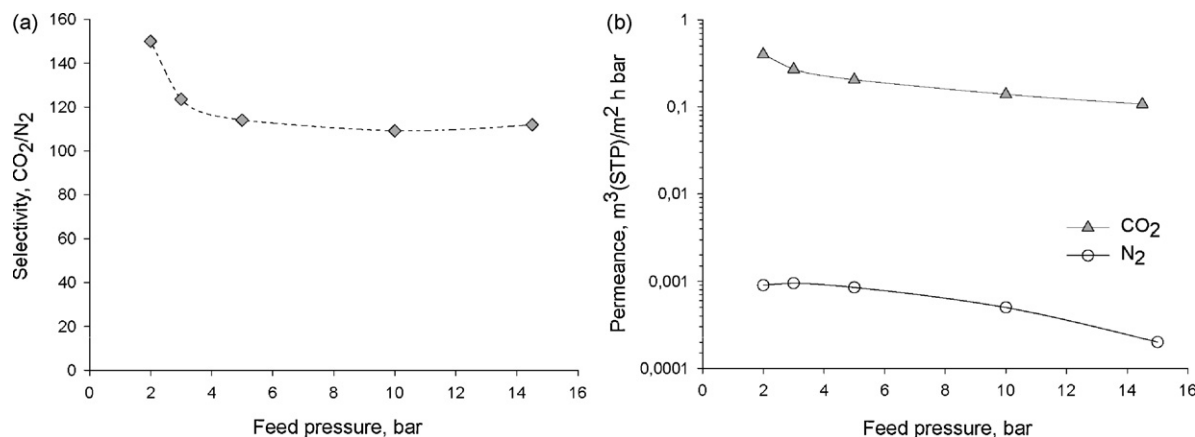


Fig. 10. Effect of feed pressure on CO₂ separation performance, selective layer of 0.5 μm , sweep gas flow rate 0.08 ml/s, at 25 °C.

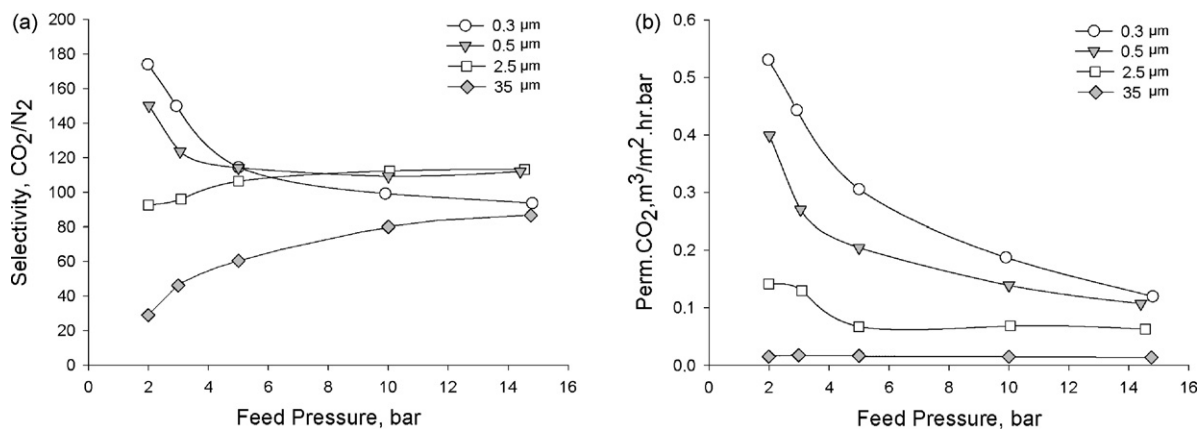


Fig. 11. Effect of feed pressure and selective layer thickness on CO₂ separation performance, selective layer 0.3 μm, 0.5 μm, 2.5 μm and 35 μm, sweep gas flow rate 0.08 ml/s, at 25 °C.

Matsuyama et al. [19] reported the separation performance of pure PVA without carriers present. They stated that the selectivity of CO₂ over N₂ in pure PVA membrane was about 70, which roughly agreed with 60 estimated by using the *S* and *D* values of CO₂ and N₂ in water. The permeance trends of CO₂ and N₂ were similar and both nearly constant when the CO₂ partial pressure was changed. Liu et al. [43] tested a series of water-swollen hydrogel membranes for CO₂ separation and also confirmed that the gas permeability in water-swollen membrane is lower than the gas permeability in water, and the selectivity of the water-swollen membranes to a pair of gases is close to the ratios of their permeabilities in water.

According to the different trends of CO₂ permeating in the blend membrane in this study and that in other water-swollen membranes we conclude that the facilitated transport mechanism dominates over the solution-diffusion mechanism in the PVAm/PVA blend membrane and primary amino groups in PVAm function as the carriers of CO₂.

3.2.3. Effect of the selective layer thickness

Fig. 11 summarizes the effect of feed pressure on CO₂ separation performance of the blend membranes as a function of selective layer thickness (note thickness 0.3 μm, 0.5 μm, 2.5 μm and 35 μm). The selectivities and permeances were recorded at their respective optimized relative humidity of the feed gas stream. At low pressure (2–3 bar), the selectivities increased dramatically with reduced selective layer thickness, whereas when feed pressure increases to around 5 bar, membranes with selective layer thicknesses of 0.3 μm, 0.5 μm and 2.5 μm exhibit similar selectivities, as shown in Fig. 11(a). At high feed pressure, however, the membrane with the thinnest selective layer shows lower selectivity. Fig. 11(b) illustrates the effect of feed pressure on CO₂ permeance as a function of membrane selective layer thickness. The membranes with thinner selective layers exhibit higher CO₂ permeances, but the effect of increasing pressure on the permeance varies. At low feed pressure (2–5 bar) the effect of thickness is much more obvious than at high feed pressure (10–15 bar). These trends suggest that the thinnest membranes (0.3 μm and 0.5 μm) are most vulnerable to the pressure effect (relatively larger permeance decrease for CO₂ than for N₂) in the low pressure region. Both CO₂ permeance and CO₂/N₂ selectivity of the blend membrane become stable when packing effect reaches the maximum of each membrane.

The competition of CO₂-carrier-mediated transport and the CO₂ Fickian diffusion may explain the phenomenon. Cussler [44] suggested a carrier-mediated transport mechanism for facilitated transport membranes. The total flux of the carrier-mediated per-

meant has been illustrated in Eq. (5):

$$J_A = \frac{D_A}{l}(C_{A,0} - C_{A,l}) + \frac{D_{AC}}{l}(C_{AC,0} - C_{AC,l}) \quad (5)$$

The first term on the right-hand side represents the Fickian diffusion while another term represents the carrier-mediated diffusion. *D_A* refers to Fickian diffusion coefficient and *D_{AC}* is the carrier-mediated diffusion coefficient of permeant-carrier complex. In this study *A* represents CO₂, *C_{A,0}* refers to the concentration of dissolved CO₂ molecules in feed side of membrane and *C_{AC,0}*, concentration of the complexed CO₂-carrier, or bicarbonate ions HCO₃⁻ in feed side of membrane. The increase of *C_{A,0}* is proportional to feed pressure and feed gas CO₂ concentration whereas *C_{AC,0}* is determined by the CO₂-carrier reaction and limited by the saturation of carriers. *C_{AC,0}* stops increasing with the feed pressure when the carriers are saturated. The thickness term, *l*, is in the denominator in Eq. (5). The smaller *l* is, the bigger the influence of terms in numerator will be. In this case the thinner selective layer leads to the more sensitive CO₂ transport competition in FSC membrane. At low pressure (before carriers are saturated), the reaction between CO₂ and carriers is fast, and the growing of *C_{AC,0}* is much faster than that of *C_{A,0}*. The CO₂ transport is dominated by facilitated transport (*C_{AC,0}* ≫ *C_{A,0}*). The thinner membranes benefit more from the competition and then exhibit better facilitated transport and hence better separation performance. At high pressure, however, when the concentration of free CO₂ is much higher than complexed CO₂-carriers (*C_{A,0}* ≫ *C_{AC,0}*), Fickian diffusion become rate-determining. In this situation thinner membrane suffers more from the loss of facilitated effect and consequently a quicker loss of CO₂/N₂ selectivity. Besides, the diffusion of N₂ is more comparable with that of CO₂ when at high pressure and without facilitated effect, which can also account for the loss of selectivity. Schultz [45] related the thickness of carrier-mediated transport membranes with the ratio between the carrier-mediated rate and the Fickian diffusion rate with the second Damköhler number, *l*²/(*Dt*_{0.5}), in which *l* is membrane thickness, *D* is the diffusion coefficient of the free component and *t*_{0.5}, half time of the complexation reaction. An optimal thickness for different operating pressures is thus possible to predict according to the Damköhler number.

3.2.4. Stability of the membrane

The lack of stability has always been a major problem concerning facilitated transport membranes. However, a very good stability has been documented for the PVAm/PVA blend membrane at 2 bar and 35 °C. Neither the carrier degradation problem nor the irreversible reaction between carriers and gases could be documented

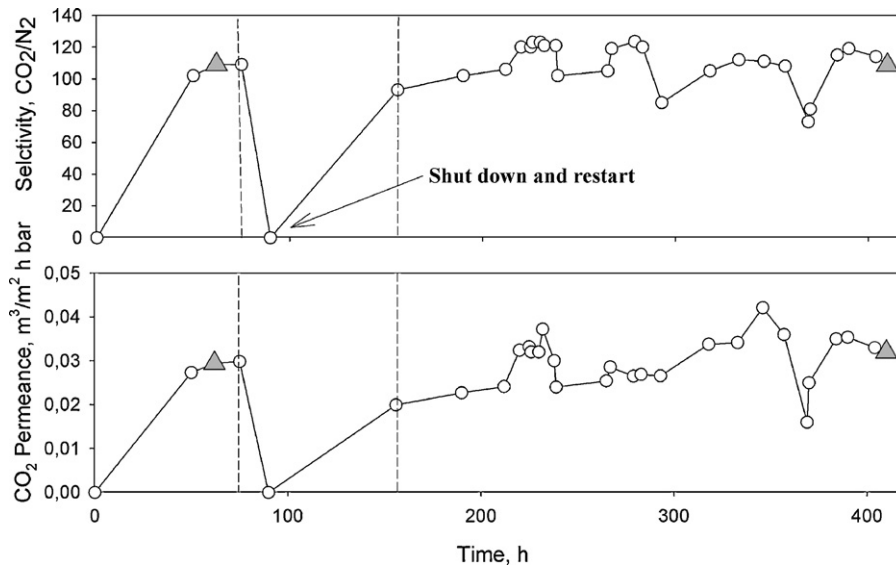


Fig. 12. Stability test of PVAm/PVA blend membrane, selective layer of 35 μm , sweep gas flow rate 0.08 ml/s.

in this blend membrane. The cross-linking and entanglement of PVAm and PVA chains, the concerted hydrophilicity of both PVA and PVAm in blend membrane also contribute to membrane stability.

Fig. 12 shows a 400 h stability test of the PVAm/PVA membrane (thickness 35 μm). During the test, separation conditions such as temperature (25–45 $^{\circ}\text{C}$), feed pressure (2–15 bar) and relative humidity (50–95%) were varied to investigate their respective effects on separation performance. A shutdown and restart process was also performed. Experiments showed the maintained separation performance at the same operation conditions at 2 bar, 35 $^{\circ}\text{C}$ before and after a 400 h run, as indicated by the two shaded triangles at the start and end of the graph in Fig. 12. As shown in the figure the membrane recovered very well after shutdown and drying for a few days, still exhibiting similar separation performance. The high water affinity of PVAm and PVA helps the blend membrane resist the deformation by cracks and defects upon exposure to dry gases for a certain period of time. The formed cracks and defects can also be cured after the swelling of the blend membrane by polymer network expanding to the surrounding near cracks and defects. The stability tests were continued more than 400 h, showing no evident loss of separation performance. This confirmed that the PVAm/PVA blend membrane was tolerable to the fluctuation of operation conditions, which is an advantage of a membrane to be used in industrial application.

The trends of separation performance of a PVAm/PVA blend membrane versus time at 10 bar, 25 $^{\circ}\text{C}$ are shown in Fig. 13. These trend lines, showing performance with time, are nearly straight after a short period (~ 60 min) and remain straight for the remaining test period (8 h) until the operation parameters were changed to 15 bar and then become straight again after a short time. It should be noted that the results reported in both Figs. 12 and 13 were obtained with a fairly thick membrane (35 μm). Recently an optimized membrane with a selective layer of 0.7 μm were tested likewise on a CO_2 – CH_4 system for more than 20 days, and then shutdown and restarted after 130 days, also showing very good stability. These results will, however, be documented in a subsequent paper concerning CO_2 / CH_4 separation.

Table 1 shows the CO_2 separation performance of membranes in this study and results of FSC membranes reported elsewhere, including CO_2 / CH_4 separation [17,46,47] and CO_2 / N_2 separation [8,16,19]. Some studies reported the ideal selectivities of CO_2 / CH_4 or CO_2 / N_2 from the permeances of pure CO_2 , N_2 or CH_4 gases [16,47] while in this study and references [8,17,19,46,48] mixed gases were utilized as feed gases. Other researchers [8,16,17,19] supplied feed gases at very low pressures and used vacuum at permeate side to reach sufficient driving forces. The results obtained at different conditions are difficult to compare. Nevertheless, the table is meant to give an overview over reported work on FSC-membranes.

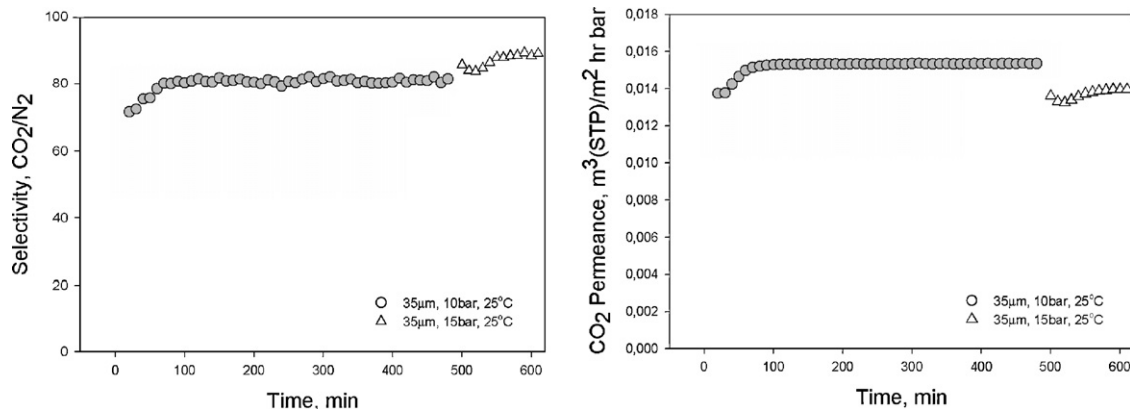


Fig. 13. Stable performance of PVAm/PVA membrane, selective layer 35 μm , sweep gas flow rate 0.08 ml/s, at 10 bar and 15 bar, 25 $^{\circ}\text{C}$.

Table 1

Comparison of membrane separation performance in current work and in other fixed-site-carrier membranes.

Membrane material	Selectivity	Permeance ($\text{m}^3(\text{STP})/(\text{m}^2 \text{ h bar})$)	Feed pressure (kPa)	Feed gas (CO_2 vol.%)	Ref.
Poly{2-(N,N-dimethyl) amino ethylmethacrylate}	130	1.6×10^{-2}	4.76	CO_2/N_2 (2.7–58%)	[8]
Poly(2-(N,N-dimethyl) aminoethoxycarbonyl)	60–90	2.7×10^{-5}	0.48	Pure CO_2 and N_2	[16]
Hydrolyzed polyvinylpyrrolidone	48	4.38×10^{-1}	1.62	CO_2/CH_4 (50%)	[17]
PEI/PVA blend	130–230	2.7×10^{-3} – 1.07×10^{-2}	6.59	CO_2/N_2 (5.8–34%)	[19]
PVAm on PS hollow fiber	53	8.2×10^{-3}	126	CO_2/CH_4 (50%)	[46]
PVAm/PEG blend	63	1.59×10^{-2}	126	Pure CO_2 and CH_4	[47]
PVAm on PSf support	200	3.0×10^{-1}	200–1500	CO_2/N_2 (10%)	[48]
PVAm/PVA blend	174–194	5.8×10^{-1} – 1.3×10^{-1}	200–1500	CO_2/N_2 (10%)	This study

In the current study, the developed blend membrane can work with feed pressures ranging from 2 bar to 15 bar and with the permeate side at atmospheric pressure. The reported results were all obtained with a gas mixture of CO_2 (10 vol.%) and N_2 (90 vol.%). The documented CO_2 permeance at 2 bar is $0.58 \text{ m}^3(\text{STP})/(\text{m}^2 \text{ h bar})$ in this study, which is nearly double of the predicted goal of $0.3 \text{ m}^3(\text{STP})/(\text{m}^2 \text{ h bar})$ for an efficient industrially feasible membrane module [49]. Selectivity of the PVAm/PVA blend membrane is comparable to or higher than other FSC membranes reported for CO_2/N_2 separation.

4. Conclusion

The composite membrane with a defect-free PVAm/PVA blend selective layer was synthesized. The CO_2/N_2 selectivity of the membrane ($0.3 \mu\text{m}$) reached 174 at 2 bar with CO_2 permeance of $0.58 \text{ m}^3(\text{STP})/(\text{m}^2 \text{ h bar})$ whereas a CO_2 permeance of $0.13 \text{ m}^3(\text{STP})/(\text{m}^2 \text{ h bar})$ was obtained with a selectivity of 94 at 15 bar. The CO_2 permeance decreased with increasing feed pressure until the carriers were saturated and the permeance became constant. This demonstrates that CO_2 is transported basically by the facilitated transport mechanism, while the transport of N_2 follows the solution-diffusion mechanism only. The performance of PVA/PVAm blend membrane can tolerate humidity fluctuation and the stability was documented over 400 h so far – experiments on a longer time scale are ongoing. In this blend membrane, PVA provides a mechanically strong polymer matrix while amino groups in PVAm function as facilitated transport carriers for CO_2 . The addition of PVA and its strong chain framework promotes a stable separation, and the good mechanical properties of the blend membrane enable the efficient ultra thin selective layer and hence much higher permeance.

PVAm/PVA blend membrane seems to be a promising membrane for CO_2 separation from gas mixtures. The membrane takes advantages of the properties of both PVAm and PVA, exhibiting high selectivity and permeability as well as good mechanical properties and stability. The good mechanical properties of the blend material are expected to make up-scaling of the membrane relatively easy. In addition, both PVA and PVAm are commercially available, and cheap polymers – the PVAm used in this study was relatively expensive 'research quality'; a product from Polyscience Inc. Today low price PVAm are easily available from producers.

Acknowledgements

The authors would like to thank the Norwegian Research Council and the Gas Centre at NTNU/Sintef for the financial support to the work. Thanks also to Prof. Raaen in the department of Physics at NTNU for the XPS analysis.

References

- [1] P.F. Scholander, Oxygen transport through hemoglobin solution, *Science* 131 (1960) 585.

- [2] O.H. LeBlanc, W.J. Ward, S.L. Matson, S.G. Kimura, Facilitated transport in ion-exchange membranes, *Journal of Membrane Science* 6 (1980) 339–343.
- [3] S.G. Kimura, W.J. Ward, S.L. Matson, Facilitated separation of a select gas through an ion exchange membrane, US Patent, 4,318,714 (1982).
- [4] J.D. Way, R.D. Noble, D.L. Reed, G.M. Ginley, L.A. Jarr, Facilitated transport of CO_2 in ion exchange membranes, *AIChE Journal* 33 (1987) 480–487.
- [5] J.J. Pellegrino, R. Nassimbene, R.D. Noble, Facilitated transport of CO_2 through highly swollen ion-exchange membranes: the effect of hot glycerine pretreatment, *Gas Separation & Purification* 2 (1988) 126–130.
- [6] H. Matsuyama, K. Hirai, M. Teramoto, Selective permeation of carbon dioxide through plasma polymerized membrane from diisopropylamine, *Journal of Membrane Science* 92 (1994) 257–265.
- [7] H. Matsuyama, M. Teramoto, H. Sakakura, K. Iwai, Facilitated transport of CO_2 through various ion exchange membranes prepared by plasma graft polymerization, *Journal of Membrane Science* 117 (1996) 251–260.
- [8] H. Matsuyama, M. Teramoto, H. Sakakura, Selective permeation of CO_2 through poly 2-(N,N-dimethyl)aminoethyl methacrylate membrane prepared by plasma-graft polymerization technique, *Journal of Membrane Science* 114 (1996) 193–200.
- [9] R. Quinn, A repair technique for acid gas selective polyelectrolyte membranes, *Journal of Membrane Science* 139 (1998) 97–102.
- [10] R. Quinn, D.V. Laciak, Polyelectrolyte membranes for acid gas separations, *Journal of Membrane Science* 131 (1997) 49–60.
- [11] R. Quinn, D.V. Laciak, G.P. Pez, Polyelectrolyte-salt blend membranes for acid gas separations, *Journal of Membrane Science* 131 (1997) 61–69.
- [12] R. Quinn, J.B. Appleby, G.P. Pez, New facilitated transport membranes for the separation of carbon dioxide from hydrogen and methane, *Journal of Membrane Science* 104 (1995) 139–146.
- [13] R. Quinn, D.V. Laciak, J.B. Appleby, G.P. Pez, Polyelectrolyte membranes for the separation of acid gases, US Patent 5,336,298 (1994).
- [14] R. Quinn, D.V. Laciak, G.P. Pez, Process for separating acid gases from gaseous mixtures utilizing composite membranes formed from salt-polymer blends, US Patent (2001).
- [15] M. Yoshikawa, K. Fujimoto, H. Kinugawa, T. Kitao, N. Ogata, Selective permeation of carbon dioxide through synthetic polymeric membrane having amine moiety, *Chem. Lett.* (1994) 243–246.
- [16] M. Yoshikawa, K. Fujimoto, H. Kinugawa, T. Kitao, Y. Kamiya, N. Ogata, Specialty polymeric membranes. V. Selective permeation of carbon dioxide through synthetic polymeric membranes having 2-(N,N-dimethyl)aminoethoxycarbonyl moiety, *Journal of Applied Polymer Science* 58 (1995) 1771–1778.
- [17] Y. Zhang, Novel fixed-carrier membranes for CO_2 separation, *Journal of Applied Polymer Science* 86 (2002) 2222–2226.
- [18] Y. Zhang, Selective permeation of CO_2 through new facilitated transport membranes, *Desalination* 145 (2002) 385–388.
- [19] H. Matsuyama, A. Terada, T. Nakagawara, Y. Kitamura, M. Teramoto, Facilitated transport of CO_2 through polyethylenimine/poly(vinyl alcohol) blend membrane, *Journal of Membrane Science* 163 (1999) 221–227.
- [20] J. Huang, J. Zou, W.S.W. Ho, Carbon Dioxide Capture Using a CO_2 -Selective Facilitated Transport Membrane, *Industrial and Engineering Chemistry Research* 47 (2008) 1261–1267.
- [21] J. Zou, W.S.W. Ho, CO_2 -selective polymeric membranes containing amines in crosslinked poly(vinyl alcohol), *Journal of Membrane Science* 286 (2006) 310–321.
- [22] Y. Cai, Z. Wang, C. Yi, Y. Bai, J. Wang, S. Wang, Gas transport property of polyallylamine-poly(vinyl alcohol)/polysulfone composite membranes, *Journal of Membrane Science* 310 (2008) 184–196.
- [23] T.J. Kim, B.A. Li, M.B. Hagg, Novel fixed-site-carrier polyvinylamine membrane for carbon dioxide capture, *Journal of Polymer Science Part B-Polymer Physics* 42 (2004) 4326–4336.
- [24] M.B. Hägg, R. Quinn, Polymeric facilitated transport membranes for hydrogen purification, *MRS Bulletin* 31 (2006) 750–755.
- [25] R.D. Noble, Generalized microscopic mechanism of facilitated transport in fixed site carrier membranes, *Journal of Membrane Science* 75 (1992) 121–129.
- [26] R.D. Noble, Analysis of ion transport with fixed site carrier membranes, *Journal of Membrane Science* 56 (1991) 229–234.
- [27] R.D. Noble, Analysis of facilitated transport with fixed site carrier membranes, *Journal of Membrane Science* 50 (1990) 207–214.
- [28] Y. Zhang, Synthesis and characteristics of novel fixed carrier membrane for CO_2 separation, *Chemistry Letters* (2002) 430–431.
- [29] Y. Zhang, Facilitated transport of CO_2 through synthetic polymeric membranes, *Chinese Journal of Chemical Engineering* 10 (2002) 570–574.

- [30] Z. Wang, M. Li, Y. Cai, J. Wang, S. Wang, Novel CO₂ selectively permeating membranes containing PETEDA dendrimer, *Journal of Membrane Science* 290 (2007) 250–258.
- [31] Wikipedia, Polyvinyl alcohol, http://en.wikipedia.org/wiki/Polyvinyl_alcohol.
- [32] M.-B. Hägg, Purification of chlorine gas with membranes—an integrated process solution for magnesium production, *Separation and Purification Technology* 21 (2001) 261–278.
- [33] J.G. Wijmans, Process PERFORMANCE = membrane properties + operating conditions, *Journal of Membrane Science* 220 (2003) 1–3.
- [34] R.K. Pinschmidt, Jr., D.J. Sagl, Polyvinylamine (overview), <http://www.polymersnetbase.com/>.
- [35] U. Goren, A. Aharoni, M. Kummel, R. Messalem, I. Mukmenev, A. Brenner, V. Gitis, Role of membrane pore size in tertiary flocculation/adsorption/ultrafiltration treatment of municipal wastewater, *Separation and Purification Technology* 61 (2008) 193–203.
- [36] B. Smitha, S. Sridhar, A.A. Khan, Synthesis and characterization of poly(vinyl alcohol)-based membranes for direct methanol fuel cell, *Journal of Applied Polymer Science* 95 (2005) 1154–1163.
- [37] M. Krumova, D. López, R. Benavente, C. Mijangos, J.M. Pereña, Effect of crosslinking on the mechanical and thermal properties of poly(vinyl alcohol), *Polymer* 41 (2000) 9265–9272.
- [38] IR-Wizard Results: 1090cm⁻¹, <http://www.science-and-fun.de/tools/>.
- [39] J.H. Kim, J.Y. Kim, Y.M. Lee, K.Y. Kim, Properties and swelling characteristics of cross-linked poly(vinyl alcohol)/chitosan blend membrane, *Journal of Applied Polymer Science* 45 (1992) 1711–1717.
- [40] G.E.P. Box, J. Stuart Hunter, W.G. Hunter, *Statistics for Experimenters*, 2nd ed., John Wiley & Sons, Inc., New Jersey, 2005.
- [41] E.L. Cussler, *Diffusion Mass Transfer in Fluid Systems*, 2nd ed., Cambridge University Press, Cambridge, 1997.
- [42] H. Matsuyama, M. Teramoto, H. Urano, Analysis of solute diffusion in poly(vinyl alcohol) hydrogel membrane, *Journal of Membrane Science* 126 (1997) 151–160.
- [43] L. Liu, A. Chakma, X. Feng, Gas permeation through water-swollen hydrogel membranes, *Journal of Membrane Science* 310 (2008) 66–75.
- [44] E.L. Cussler, in: D.R. Paul, Y.P. Yampol'skii (Eds.), *Polymeric Gas Separation Membranes*, CRC Press, Boca Raton, 1993 (chapter 6).
- [45] J.S. Schultz, J.D. Goddard, S.R. Suchdeo, Facilitated transport via carrier-mediated diffusion in membranes. I. Mechanistic aspects, experimental systems and characteristic regimes, *AIChE Journal* 20 (1974) 417–445.
- [46] C.M. Dong, Z. Wang, C.H. Yi, S.C. Wang, Preparation of polyvinylamine/poly sulfone composite hollow-fiber membranes and their CO₂ separation performance, *Journal of Applied Polymer Science* 101 (2006) 1885–1891.
- [47] C. Yi, Z. Wang, M. Li, J. Wang, S. Wang, Facilitated transport of CO₂ through polyvinylamine/polyethylene glycol blend membranes, *Desalination* 193 (2006) 90–96.
- [48] M.B. Hägg, R. Quinn, Membrane for carbon sequestration and offer environmental application, in: *Petrobras International Seminar*, Rio de Janeiro, 2006.
- [49] M.B. Hägg, A. Lindbrathen, CO₂ capture from natural gas fired power plants by using membrane technology, *Industrial and Engineering Chemistry Research* 44 (2005) 7668–7675.